

# Notes on the videotape

## **Nonlinear Dynamics and Chaos: Lab Demonstrations**

by Steven H. Strogatz

For more information, please write to me at Kimball Hall, Theoretical and Applied Mechanics, Cornell University, Ithaca, NY 14853, or send e-mail to [strogatz@cornell.edu](mailto:strogatz@cornell.edu)

Please copy the videotape and give it to anybody who might be interested. Also, please send the tape back to me after you've copied it, so I can send it to other people.

These notes are intended to summarize the main points in the tape, to provide background where necessary, and to underscore the dynamical concepts that are being demonstrated.

### **1. Chaotic Waterwheel**

(with Howard Stone, Division of Applied Sciences, Harvard)

A tabletop waterwheel, designed and built by Prof. Willem Malkus (Math. Dept., MIT), is used to demonstrate chaos in a mechanical analog of the Lorenz equations. The waterwheel's rotational damping rate can be adjusted by tightening or loosening a brake. When the brake is not too tight, the wheel settles into a steady rotation. Either direction of rotation is possible.

When the brake was tightened in an attempt to make the wheel go chaotic, unfortunately it was tightened too much. Instead of settling into the desired pattern of irregular reversals, the wheel fell into a simple pendulum-like motion, turning once to the left, then back to the right, and so on. After the brake was loosened slightly, the motion became chaotic. (And the crowd went wild...)

The waterwheel is an exact mechanical analog of the Lorenz equations (see Exercise 9.1.3 in Strogatz (1994)). The corresponding Lorenz parameters are  $b = 1$ ,  $\sigma \propto \nu$ , and  $r \propto \nu^{-1}$ , where  $\nu$  is the rotational damping rate. So as the brake is tightened, the parameters are constrained to move along a hyperbola  $r\sigma = C$  in the  $(r, \sigma)$  parameter space.

Reference: Section 9.1 of S.H. Strogatz, *Nonlinear Dynamics and Chaos*, Addison-Wesley (1994).

## 2. Double Pendulum

(with Howard Stone, Division of Applied Sciences, Harvard)

A double pendulum is used to illustrate some basic ideas about chaos in Hamiltonian systems. The small-amplitude motion of the double pendulum consists of in-phase or antiphase normal modes, or linear combinations of these two modes. The resulting motion is tame: either periodic or quasiperiodic with two frequencies.

But large-amplitude motions can be spectacular. The motion is chaotic if the pendula are released from rest, starting from a configuration where both pendula are horizontal but in antiphase. In contrast, if the pendula are released from a horizontal *in-phase* configuration, the motion is merely quasiperiodic. Both initial conditions have the same total energy, yet the antiphase initial condition leads to much more complicated dynamics. This shows that the complexity of the motion depends on more than just its energy. (This demonstration also illustrates the idea of a “divided phase space” in a Hamiltonian system; chaotic solutions and quasiperiodic solutions can co-exist on the same energy shell.)

To show that chaotic motions depend sensitively on initial conditions, two (nearly) identical pendula were released from (nearly) the same antiphase initial condition. The pendula swung in unison for a while (this is interesting to watch in slow motion, if you have that setting on your VCR) but soon their motions became totally different.

Reference: T. Shinbrot, C. Grebogi, J. Wisdom, and J.A. Yorke, “Chaos in a double pendulum”, *American Journal of Physics* **60**, 491 (June 1992).

## 3. Airplane Wing Vibrations

(with John Dugundji, Dept. of Aeronautics and Astronautics, MIT)

These demonstrations of aeroelastic instabilities serve at least two purposes. They illustrate some fundamental ideas in nonlinear dynamics, including stable and unstable fixed points, limit cycles, subcritical and supercritical Hopf bifurcations, and coexistence of attractors. They also connect nonlinear dynamics to real-world phenomena -- see the NASA footage at the end of this segment of the video.

### 3.1 *Single degree-of-freedom system*

A small wind tunnel is used in the lab demonstrations. There is a variable-speed fan at the left end of the wind tunnel. The fan is pointed outward, sucking air through the tunnel from right to left. The experiments are performed on a wing that is pivoted about its mid-chord so that it has only a torsional degree of freedom. The wing is restrained by a linear torsional spring (not visible in the video) that can be biased to provide the wing with various initial angles of attack.

The leading edge of the wing is marked by a dot, and there are angle lines marked on the board behind the wing to aid in quantifying the wing's motion.

### 3.1.1 *Angle of attack = 0°.*

In the absence of any wind, if the wing is disturbed slightly, its free vibrations are underdamped. (The eigenvalues are complex and in the left half plane.) When the wind is turned on, at around 10-15 ft/sec the wing is still stable at the horizontal position (0° angle of attack), but now its free vibrations take much longer to decay. The wind has caused the eigenvalues to move closer to the imaginary axis. The system is becoming less stable.

At a wind speed  $V \approx 18$  ft/sec, the wing still has a stable angle of attack, but now it has rotated to around 5°. A sufficiently large disturbance sends the wing into a violent oscillation, corresponding to a large-amplitude limit cycle. However, small disturbances die out. This shows that the system has two co-existing attractors: a large-amplitude limit cycle, and a static equilibrium at around 5°. This coexistence is one of the hallmarks of an impending *subcritical Hopf bifurcation* (the mechanism by which the static state will go unstable at a slightly higher wind speed.)

For a wind speed a little above 18 ft/sec, the static state loses stability and the wing spontaneously goes into a limit cycle with fluctuations of  $\pm 90^\circ$  (keep your eye on the white dot to see this). At even higher wind speeds, the amplitude is about  $\pm 120^\circ$ . As the wind speed is brought back down, the amplitude of the limit cycle appears to decrease continuously, at least for a while, and then the wing jumps back to static equilibrium.

### 3.1.2 *Angle of attack = 5°*

By adjusting the torsional spring, the initial angle of attack is now biased to 5°. When the wind is turned on, the wing immediately rotates to a new static position (unlike the experiments above, where the wing stayed near its initial 0° over a range of wind speeds.)

At  $V \approx 17$  ft/sec, we find a number of remarkable phenomena. First of all, the wing starts jiggling slightly. This low-amplitude limit cycle is completely different from the violent oscillations seen earlier -- it is born in a *supercritical Hopf bifurcation*. Furthermore, it's a self-excited vibration; it doesn't need a kick to get it started.

At the same wind speed, a large kick sends the wing into a violent oscillation of  $\pm 70^\circ$ . Therefore, at  $V \approx 17$  ft/sec the system has *two* co-existing stable limit cycles. (You should think about what the phase portrait would look like.)

Finally, when the large-amplitude vibration is manually suppressed, the system spontaneously reverts to the small-amplitude cycle.

## 3.2 *Two degree-of-freedom system*

This system has both bending and torsional degrees of freedom; it can move up and down, as well as rotate. It is therefore more like a section of an airplane wing, whereas the single degree-of-freedom airfoil used earlier is more like a turbine blade.

Without any wind, the free vibrations are underdamped for both torsional and bending

motions. At a wind speed of 20 ft/sec, the vibrations take much longer to die down, but the wing is still stable.

At  $V = 25$  ft/sec, the static equilibrium is still stable to very small disturbances, but a sufficient kick brings the system into a limit cycle that combines torsional and bending oscillations (so again we have two co-existing attractors). Next a somewhat smaller kick is used, one that is just barely large enough to trigger the oscillations. Note how the oscillations build up before saturating at their final amplitude. When a tiny kick is used, nothing much happens; the wing goes back to equilibrium. Finally, at high wind speed, the wing is easily kicked into a violent oscillation.

### 3.3 *Real airplanes*

This marvelous and unintentionally campy footage shows some scenes from a NASA film about aeroelastic phenomena (NASA 1973). One scene shows a small airplane undergoing tail flutter, and another shows a sailplane exhibiting, in the words of the announcer, "...classical aileron flutter. The aileron motion couples with wing bending."

In a part of the film that we edited out (but shouldn't have), the announcer emphasizes that commercial airplanes are carefully designed and tested to ensure that these dangerous vibrations could *never* occur under normal conditions, so you shouldn't worry.

#### References:

K. Aravarnudan and J. Dugundji, "Stall flutter and nonlinear divergence of a two-dimensional flat plate", Aeroelastic and Structures Research Laboratory, MIT, Cambridge, Massachusetts, ASRL-TR-159-6, Air Force Office of Scientific Research, AFOSR-TR-74-1734, July 1974.

E.H. Dowell and M. Ilgamova, *Studies in Nonlinear Aeroelasticity*, Springer-Verlag (1988).

NASA Technical Film Serial L-1 128, "Aeroelastic phenomena and related research", NASA Langley Research Center, Hampton, VA 23365, June 1973.

Section 8.2 of S.H. Strogatz, *Nonlinear Dynamics and Chaos*, Addison-Wesley (1994).

## 4. **Chemical Oscillators**

(with Irving Epstein, Chemistry Dept., Brandeis University)

The Briggs-Rauscher reaction is an oscillating chemical reaction that cycles between blue (oxidized) and yellow (reduced) states. Its recipe is given below, courtesy of Irving Epstein:

Three solutions are required:

- A. 0.14M  $\text{KIO}_3$
- B. 3.2M  $\text{H}_2\text{O}_2$  (start from 30% solution)  
0.17M  $\text{HClO}_4$
- C. 0.15M malonic acid ( $\text{CH}_2(\text{COOH})_2$ )  
0.024M  $\text{MnSO}_4$   
10g/l soluble starch

Mix equal volumes of A, B, C and stir.

The system is closed and so it eventually goes to thermodynamic equilibrium, but en route it oscillates between blue and yellow states. As the demonstration proceeds, the reaction spends more and more time in the blue state, and so the oscillation period gradually lengthens. Finally, when the magnetic stirrer is turned off, the system spends a distressingly long time in the blue state before finally changing color again. During the transition, notice the spatial structure in the system, made possible by the lack of stirring.

#### References:

T.S. Briggs and W.C. Rauscher, *Journal of Chemical Education* **50**, 496 (1973).

I.R. Epstein, K. Kustin, P. De Kepper, and M. Orban, "Oscillating chemical reactions", *Scientific American* **248** (3), 112 (1983).

Section 8.3 of S.H. Strogatz, *Nonlinear Dynamics and Chaos*, Addison-Wesley (1994).

## **5. Synchronized Chaos and Private Communications**

(with Kevin Cuomo, MIT Lincoln Laboratory)

Using an analog circuit implementation of the Lorenz equations, this demonstration shows that two chaotic systems can become synchronized. The demonstration also indicates that chaos might have the potential to be useful in certain applications to private communications (although it is still too early to tell just how useful it might be; the work described here is only a few years old, and there are many competing methods that are well-established and tested).

### **5.1 Lorenz circuit**

First a single Lorenz circuit is studied. The plot on the oscilloscope screen shows  $x(t)$  vs.  $z(t)$ , and the trace resembles the familiar strange attractor for the Lorenz system. The Lorenz parameters  $r$ ,  $\sigma$ , and  $b$  can be varied independently by adjusting the corresponding variable resistor in the circuit. As one of these resistors is varied, the circuit is seen to exhibit a sequence

of different attractors: first a fixed point, then a small-amplitude limit cycle that grows continuously out of the fixed point (indicating that a supercritical Hopf bifurcation has occurred), then a period-doubled limit cycle, then a strange attractor of Rössler type, and finally a Lorenz attractor.

In addition to being seen, the attractors and bifurcations can also be heard -- when the signal  $x(t)$  is played through a loudspeaker, the limit cycle sounds like a pure tone. When period-doubling occurs, another tone becomes audible, about an octave higher. The Rössler and Lorenz attractors sound noisy, as expected for chaotic signals.

If you find it hard to believe this bifurcation sequence, see footnote 5.4 below. But for most readers, it is probably better not to be distracted by footnote 5.4 at this stage.

## 5.2 Synchronized chaotic circuits

Now two nearly identical Lorenz circuits are studied; one acts as the transmitter and the other as the receiver. The transmitter parameters are such that the circuit is in the Lorenz chaotic regime. The transmitter signal  $x(t)$  is fed into the receiver in a certain way, with the result that the receiver quickly synchronizes to the transmitter, starting from any initial conditions (see below for mathematical details). This synchronization is demonstrated experimentally by plotting  $x(t)$  vs. the corresponding receiver variable  $x_r(t)$ . The oscilloscope trace shows a blurry 45° diagonal line, indicating that  $x(t) \approx x_r(t)$ . The blur is visibly reduced when the transmitter's parameters are tuned to match the receiver's. You can also hear the improvement -- when the synchronization error  $e_x(t) = x(t) - x_r(t)$  is played through the loudspeaker, the hiss gets quieter as the tuning improves. Similar results would be obtained for the other state variables  $y(t)$  and  $z(t)$ .

In more mathematical detail, the governing equations for the transmitter are

$$\begin{aligned}\dot{x} &= \sigma(y - x) \\ \dot{y} &= rx - y - xz \\ \dot{z} &= xy - bz\end{aligned}$$

while the receiver's state  $(x_r, y_r, z_r)$  evolves according to

$$\begin{aligned}\dot{x}_r &= \sigma(y_r - x_r) \\ \dot{y}_r &= rx(t) - y_r - x(t)z_r \\ \dot{z}_r &= x(t)y_r - bz_r\end{aligned}$$

Notice that the transmitter signal  $x(t)$  is fed into the second and third equations of the receiver. Also, the receiver has the same parameter settings  $r, \sigma, b$  as the transmitter. One can prove that the receiver synchronizes with the transmitter, in the sense that  $\mathbf{x}_r(t) \rightarrow \mathbf{x}(t)$  as  $t \rightarrow \infty$ , where  $\mathbf{x} =$

$(x, y, z)$  and  $\mathbf{x}_r = (x_r, y_r, z_r)$ . The synchronization is exponentially fast for all initial conditions. The proof uses a Liapunov function for the difference dynamics -- see Cuomo and Oppenheim (1993) and Strogatz (1994).

Some people are surprised to learn that chaotic systems can synchronize, despite their sensitive dependence on initial conditions. This oft-mentioned “paradox” is based on a misunderstanding -- sensitive dependence holds only for the *uncoupled* systems. When driven by the transmitter, the receiver is actually completely *insensitive* to its initial conditions, in the sense that  $\mathbf{x}_r(t)$  always converges to  $\mathbf{x}(t)$ , no matter what the initial conditions are.

### 5.3 Application to private communications

Suppose you want to send a private message over the airwaves to a friend. For instance, Princess Diana might have preferred more privacy when she whispered sweet nothings to her boyfriend James Gilbey over a cellular phone, only to find those conversations later reported in the media as the embarrassing “Squidgy” tapes. One approach would be to mask that message with much louder static, so that an eavesdropper would only hear the static, and would have a hard time detecting the underlying message. Of course, for this “signal masking” approach to be useful, James needs to have a way of subtracting off the static covering Diana’s message.

That’s where synchronized chaos comes in. Diana has the transmitter and James has the receiver. They agree to use the same parameter values (which could be changed from day to day), but he doesn’t know what message she’s going to send. Suppose  $m(t)$  is her message signal and the chaotic transmitter signal  $x(t)$  is the much louder mask. The hybrid signal  $s(t) = m(t) + x(t)$  is sent over the airwaves and used to drive James’s receiver, i.e.,  $s(t)$  replaces  $x(t)$  in the receiver dynamics above. The hope is that the variable  $x_r(t)$  regenerated at the receiver will be close enough to  $x(t)$  that it can be used in place of the unknown original mask. Then subtracting  $x_r(t)$  from  $s(t)$  gives an estimate of the message:  $\hat{m}(t) = s(t) - x_r(t)$ .

The demonstration tests this approach in real circuits, although wires are used in place of the airwaves. The song “Emotions” by Mariah Carey is used as the message signal  $m(t)$ . After hearing the original, we next hear the hybrid signal  $s(t)$ , which sounds like a meaningless hiss because the music is buried under the chaotic mask. On the oscilloscope trace, we see  $x(t)$  vs.  $x_r(t)$ . The diagonal line indicates that the receiver and transmitter circuits are maintaining synchronization. Departures from the diagonal occur whenever the music is relatively loud -- notice that the beat of the music is visible in the fluctuations. Finally, when the reconstructed message  $\hat{m}(t)$  is played, we hear the song again, although it’s a little fuzzy because  $x_r(t)$  is not a perfect reproduction of  $x(t)$ . (In fact, the synchronization error is comparable to the message itself, which leads one to wonder why the signal recovery works at all. See Cuomo, Oppenheim, and Strogatz (1993) for an analysis of this issue.)

### 5.4 A footnote for experts

As soon as we finished taping this demonstration, we realized we had seen some unexpected phenomena in Demonstration 5.1. For instance, the nontrivial fixed points in the Lorenz system

are normally supposed to lose stability in a subcritical, not a supercritical, Hopf bifurcation. Hence it was a surprise to see a small stable limit cycle bifurcating from the fixed point. And the period-doubling route to chaos is not the standard route in the Lorenz system.

Here is our best guess at the explanation. We know that the parameter values used were *not* the traditional values  $\sigma = 10$  and  $b = 8/3$  (where  $r$  is adjustable). In the original experiments reported in Cuomo and Oppenheim (1993), the parameters were  $r = 45.6$ ,  $\sigma = 16$ , and  $b = 4$ , but those experiments took place many months before this video was made, and some of the circuit components may have drifted. Furthermore, it appears now that Cuomo may have been varying  $b$ , not  $r$  as claimed in the tape. Finally, the circuit equations may need to include an imperfection term  $\varepsilon \approx 0.01$ , caused by a small but measurable voltage offset at the output of the two analog multipliers in the circuit. With this effect included, and with the equations scaled as in Cuomo and Oppenheim (1993), the circuit equations become

$$\begin{aligned}\dot{x} &= \sigma(y - x) \\ \dot{y} &= rx - y - 20(xy + \varepsilon) \\ \dot{z} &= 5(xy + \varepsilon) - bz\end{aligned}$$

This  $\varepsilon$  term breaks the symmetry  $(x,y) \rightarrow (-x,-y)$  of the Lorenz equations, but it does *not* affect the synchronization performance of the circuits.

Numerical simulations with  $r = 45.6$ ,  $\sigma = 16$ ,  $\varepsilon = 0.01$  show all the phenomena seen in the video. There is a supercritical Hopf bifurcation at  $b = 0.4028$ , a stable limit cycle for  $b = 0.5$ , a period-doubled limit cycle for  $b = 0.65$ , and a Rössler attractor for  $b = 0.68$ , all as observed on the oscilloscope.

Despite any remaining uncertainties about the equations governing the circuit on the day that the video was made, it is clear that the system still worked! The chaotic circuits successfully synchronized, and the Mariah Carey song was successfully masked, transmitted, and recovered.

#### References:

- K.M. Cuomo and A.V. Oppenheim, "Circuit implementation of synchronized chaos with applications to communications", *Physical Review Letters* **71**, 65 (1993).
- L.M. Pecora and T.L. Carroll, "Synchronization in chaotic systems", *Physical Review Letters* **64**, 821 (1990).
- K.M. Cuomo, A.V. Oppenheim, and S.H. Strogatz, "Robustness and signal recovery in a synchronized chaotic system", *International Journal of Bifurcation and Chaos* **3**, 1629 (1993).

Section 9.6 of S.H. Strogatz, *Nonlinear Dynamics and Chaos*, Addison-Wesley (1994).

## 6. Musical Variations from a Chaotic Mapping

(with Diana Dabby, Department of Electrical Engineering, MIT)

Diana Dabby has developed a chaotic mapping for generating musical variations of an original work (Dabby 1995). In this demonstration, the method is applied first to Bach's Prelude in C Major, from the Well-Tempered Clavier, Book I, and then to Gershwin's Prelude 1.

Since Diana explains her artistic motivation very clearly on the videotape, and the variations speak for themselves, the only remaining thing to do here is to explain how the method works. The Lorenz equations are integrated numerically, starting from some reference initial condition. Let the sequence  $\{x_i\}$  denote the  $x$ -values obtained after each time step. Each  $x_i$  is then paired with a pitch  $p_i$  from the pitch sequence  $\{p_i\}$  of the notes or chords heard in the original piece (Figure 1). The first pitch  $p_1$  is assigned to  $x_1$ , and  $p_2$  is assigned to  $x_2$ , and so on, continuing until each pitch has been assigned a value of  $x$ .

Figure 1 shows a small subset of the  $x$ -axis configured in this way, with the corresponding pitches plotted along it like fenceposts. For clarity, only five points are shown. In practice, the method might involve hundreds of points along the  $x$ -axis.

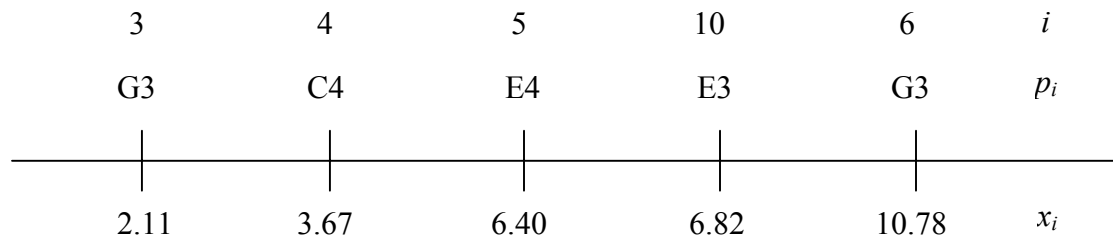


Figure 1.

To generate a variation, a trajectory is started from a different initial condition. Let  $x'_j$  denote its  $x$ -components after successive time steps in the numerical integration. For each  $x'_j$ , assign it the pitch  $p_{g(j)}$ , where  $g(j)$  denotes the index  $i$  of the smallest  $x_i$  such that  $x_i \geq x'_j$ . To express this rule in more visual terms, imagine that the original pitches  $p_i$  define a musical landscape along the  $x$ -axis, as in Figure 1 above. The rule says that each  $p_i$  controls the interval of the  $x$ -axis between itself and the pitch to its immediate left. Then when a new trajectory comes along, its components  $x'_j$  fall into these various intervals, thereby triggering the pitches at the righthand endpoints and generating a variation. As a hypothetical example, if  $x'_5 = 6.53$ , then the new pitch  $p'_5$  would be E3, whereas if  $x'_5 = 6.38$ , then the new pitch  $p'_5$  would be E4, the same as  $p_5$  in the original piece.

It may be helpful to think of the method this way: the mapping takes the original music and maps it onto the back of the strange attractor. The temporal sequence of pitches is linked to the temporal sequence of points along a certain Lorenz trajectory. When a new trajectory is launched, it travels through this musical landscape in a different way, thereby generating a

variation. But because the landscape incorporates features of the original musical piece, the resulting variations tend to evoke the source.

The method tempers the variations in several ways. For instance, only pitch is varied, and no variation can include a pitch not present in the original. By extending the mapping to the  $y$  and  $z$  axes, variations could be generated that differ in rhythm and loudness as well as pitch. Other factors affecting the extent and nature of variation are the choice of initial condition, step length, length of integration, and the amount of truncation and round-off applied to the trajectories.

References:

D.S. Dabby, "Musical variations from a chaotic mapping", *Chaos* **6**, 95 (1996).

I. Peterson, "Bach to chaos: Chaotic variations on a classical theme", *Science News* **146**, 428 (December 24 & 31, 1994).